

YMTHE, Volume 26

Supplemental Information

Immunological Synapse Predicts Effectiveness of Chimeric Antigen Receptor Cells

Wei Xiong, Yuhui Chen, Xi Kang, Zhiying Chen, Peilin Zheng, Yi-Hsin Hsu, Joon Hee Jang, Lidong Qin, Hao Liu, Gianpietro Dotti, and Dongfang Liu

Supplementary Figures

Figure S1

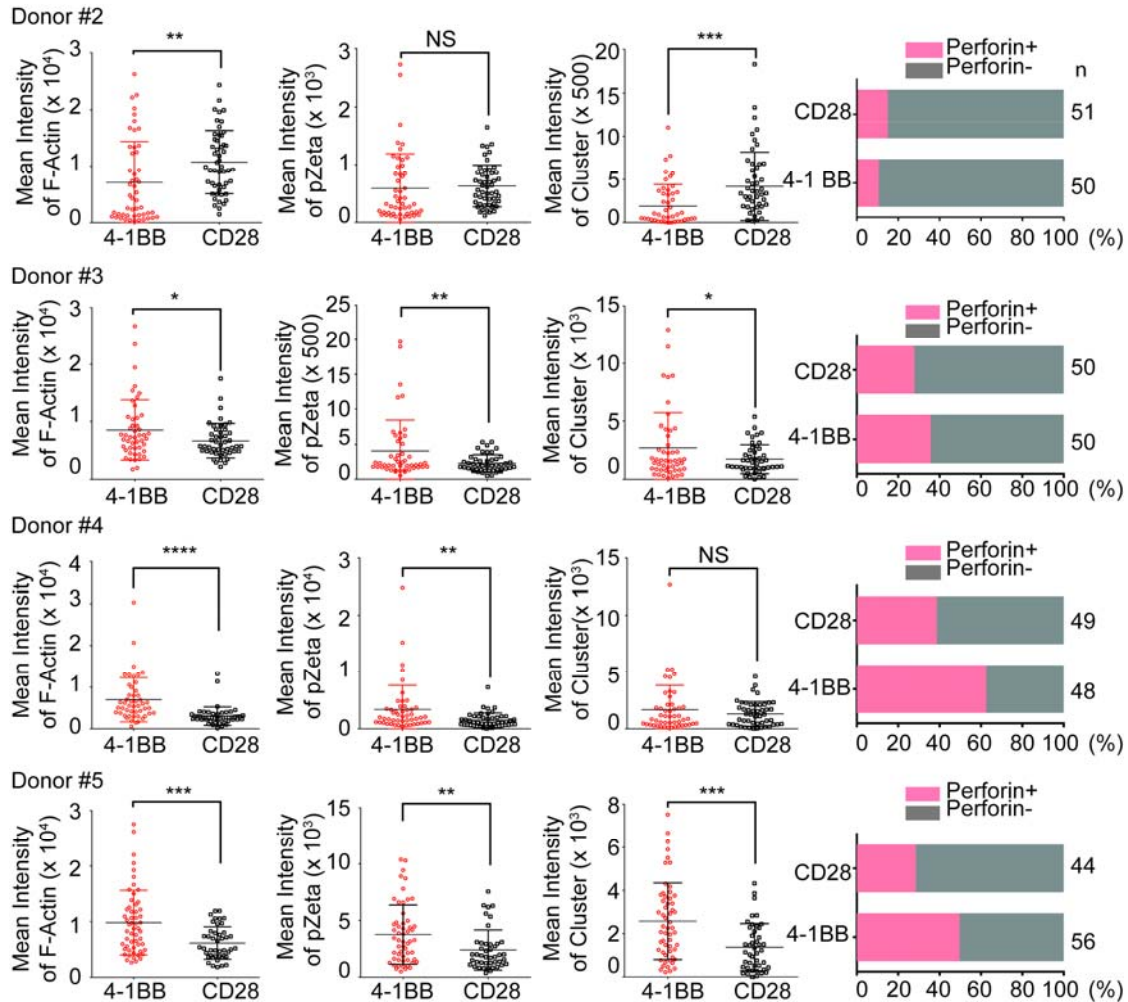


Figure S1: Quantification of IS quality. CAR T cells were added to the lipid bilayer containing Alexa Fluor 647 labeled Kappa IgG1. Cells were stained with Abs against perforin, pZeta, and phalloidin (F-actin staining). The IS under the lipid bilayer was quantified by measuring the mean fluorescence intensities of F-actin, pZeta, and Kappa cluster, as well as the percentage of perforin-positive cells on the glass-supported planar lipid bilayer containing Kappa IgG1. Error bars show \pm standard deviation (s.d.). NS, not significant.

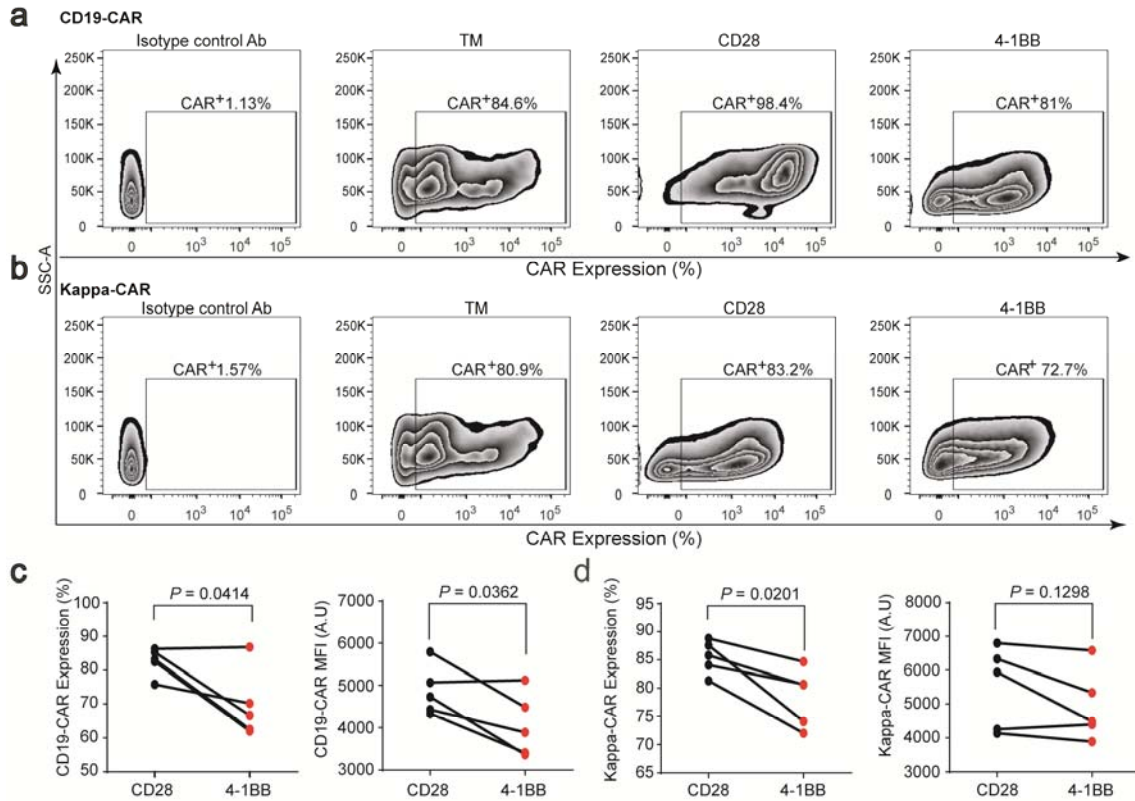


Figure S2: Comparison of CAR expression and transduction efficiencies between CD28-CAR and 4-1BB-CAR. (a) Representative flow cytometry analysis of Kappa-CAR and CD19-CAR expression on the surface of T cells from one of individuals. TM-control CAR (TM), as well as isotype control, is displayed (left panel). Gating was based on the isotype controls. (b) Statistical comparison of CAR expression between CD28-CAR and 4-1BB-CAR. PBMCs from five individuals were transduced with 4-1BB construct (red dots) or CD28 construct (black dots) retrovirus. Five days after transduction, flow cytometry was performed to analyze the CAR expression. This data represents at least three independent experiments. *P* value is for paired t-test.

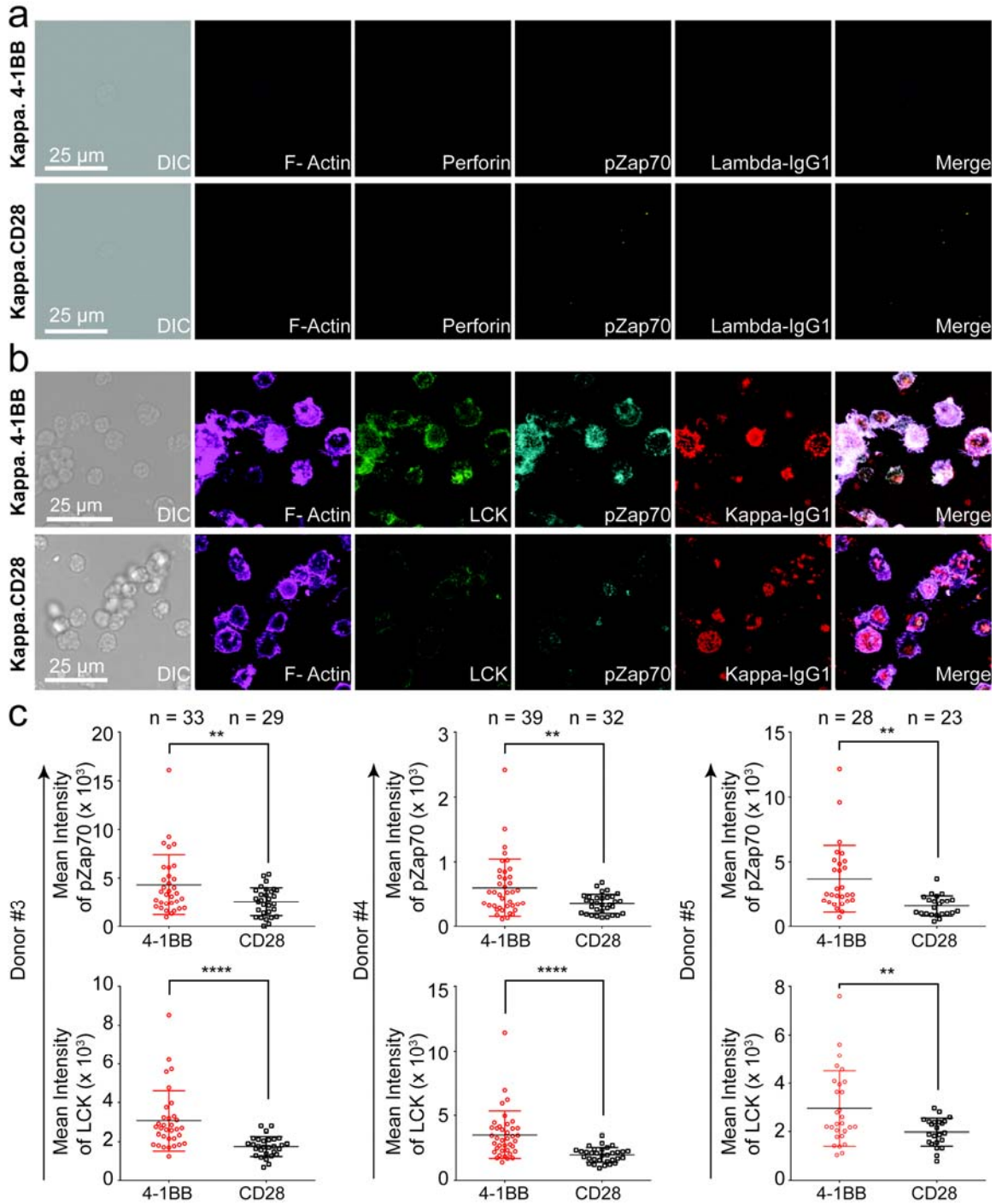


Figure S3: Specific interactions between Kappa-CAR T cells and the lipid bilayer carrying Kappa antigen. (a and b) Representative confocal images of 4-1BB- and CD28-CAR T cells. CAR T cells on the lipid bilayer carrying Alexa Fluor 647-labeled Lambda IgG1 (a, as a control for kappa antigen) or Alexa Fluor 647- labeled Kappa IgG1 (b, tumor antigen). Fixed CAR T cells were stained for perforin, pZap70, LCK, and F-actin, as indicated. Scale bars represent 25.0 μ m. (c) Quantification of the mean fluorescence intensities of F-actin, pZAP70, and cluster of Kappa. Error bars show \pm s.d.

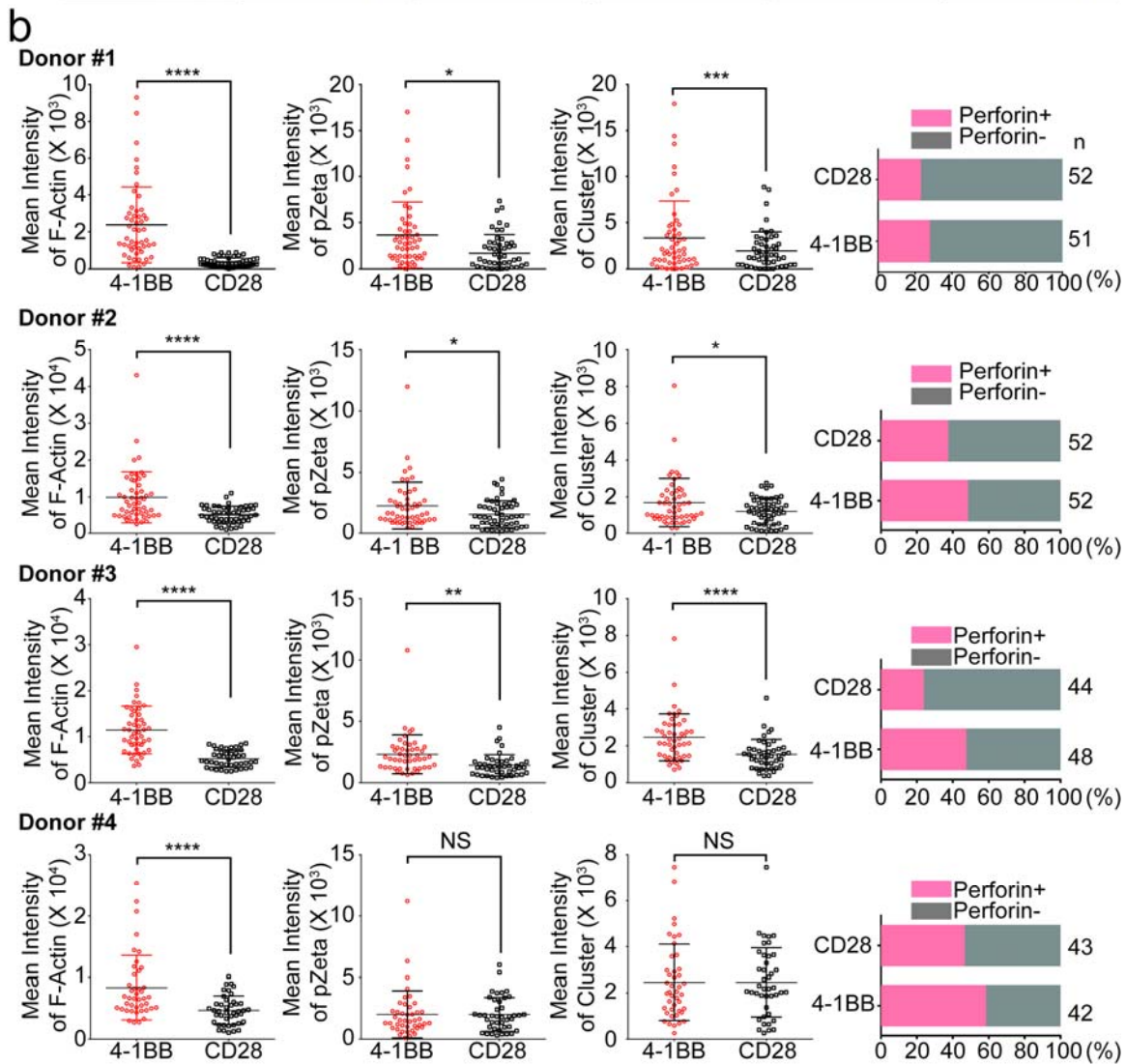
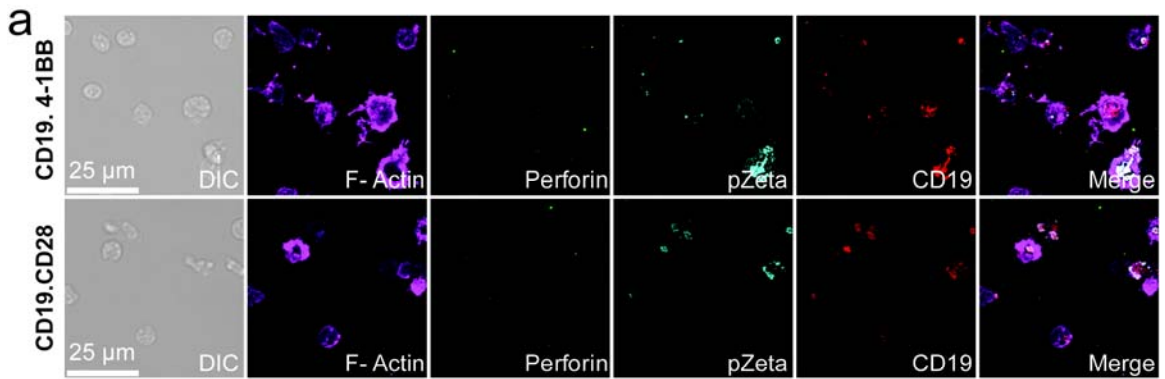


Figure S4: Superior IS quality in CD19 specific 4-1BB-CAR T cells. (a) Representative confocal microscopy of CD19-CAR T cells with 4-1BB or CD28

activated on lipid bilayer carrying CD19-Alexa Fluor 568 (red). Fixed and permeabilized CD19-CAR T cells were stained for perforin and pZeta. Then, these cells were incubated with phalloidin, Alexa Fluor 532 (magenta), Alexa Fluor 647-(green), and Alexa Fluor 488-(cyan) conjugated secondary Abs, respectively. Scale bars represent 25.0 μm . **(b)** Quantification of the IS quality under the lipid bilayer obtained by measuring the mean fluorescence intensities of F-actin, pZeta, and CD19 cluster, as well as the percentage of perforin-positive cells on the lipid bilayer containing CD19. Error bars show \pm s.d.

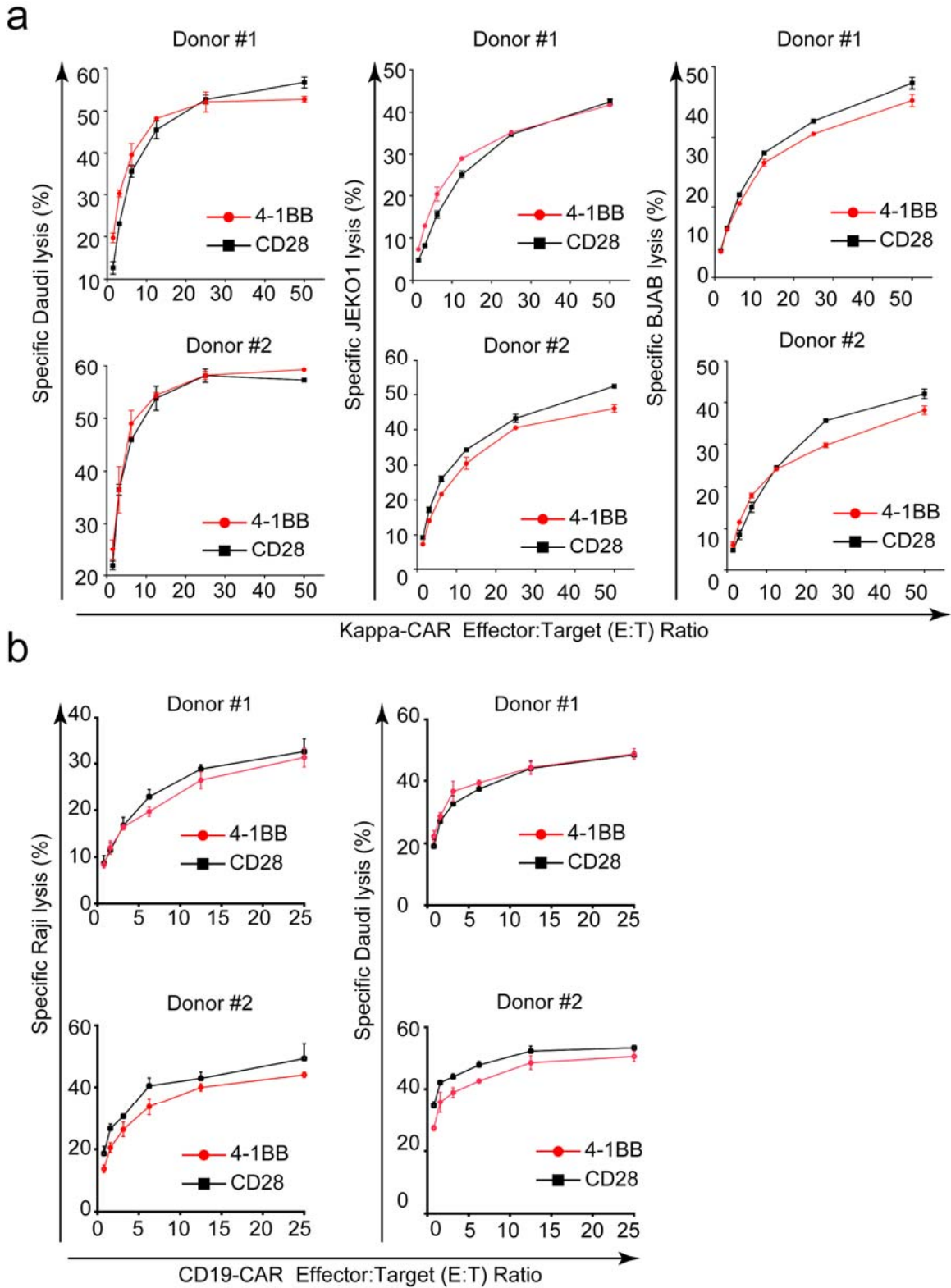


Figure S5: Standard ^{51}Cr release assay cannot distinguish the difference between 4-1BB-CAR and CD28-CAR from cytotoxicity of CAR T cell to multiple tumor cell lines. The cytotoxicity of Kappa-CAR T (a) and CD19-CAR (b) cells from two

individuals (Donor #1 and Donor #2) was measured using a standard 4-h ^{51}Cr -release assay. Three Kappa positive B-cell lymphoma cell lines (Daudi, JEKO1, and BJAB) were used as Kappa-CAR T cell's target cells. The two CD19 positive B- cell lymphoma cell lines (Daudi and Raji) were used as the target cells. Error bars show \pm s. d. PBMCs from individuals were transduced with 4-1BB construct (red dots) or CD28 construct (black dots) retrovirus, as described in Figure 1.

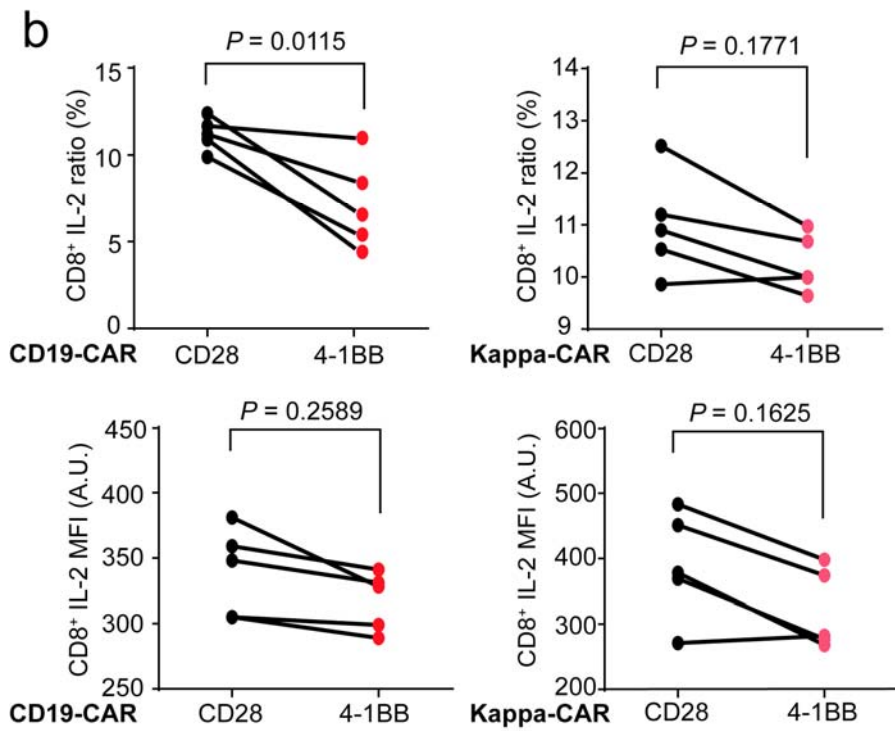
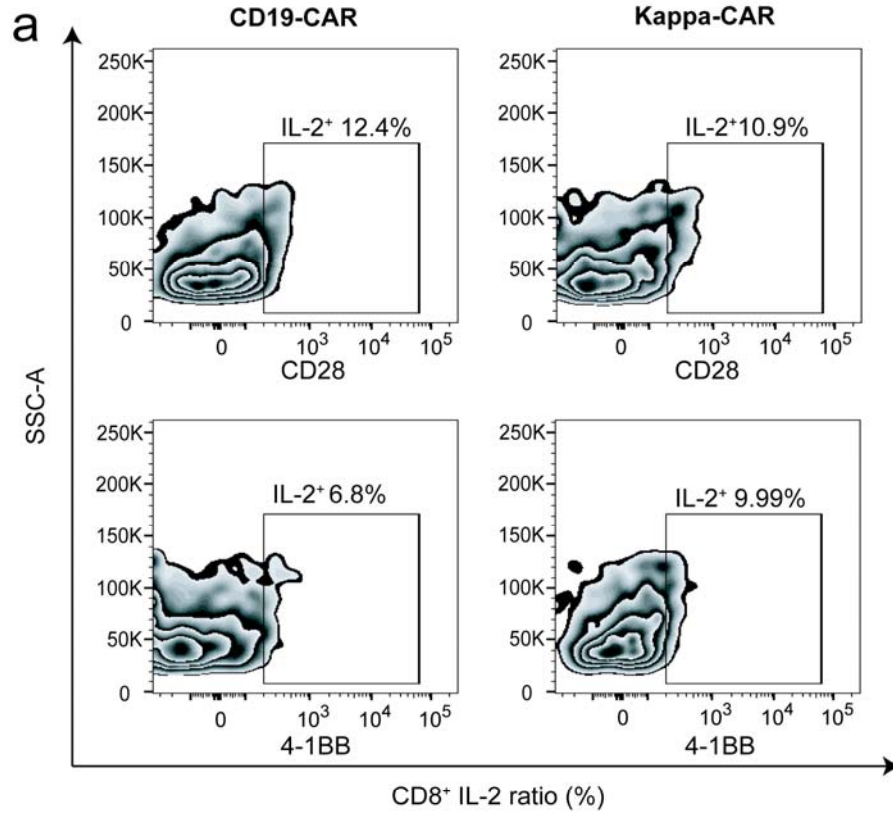


Figure S6: Comparable IL-2 expression between CD28-CAR T and 4-1BB-CAR T cells.

(a) Representative flow cytometry analysis of IL-2 expression in CD8 positive population from CD28- and 4-1BB-CAR T cells (CD19-CAR and Kappa-CAR). (b) PBMCs from five donors transduced with 4-1BB-CAR (red dots) or CD28-CAR (black dots), respectively. The ratio (%) and expression (MFI) of IL-2 in CD8 subset were calculated. This data is pooled from at least two independent experiments. *P* value is for paired t-test.

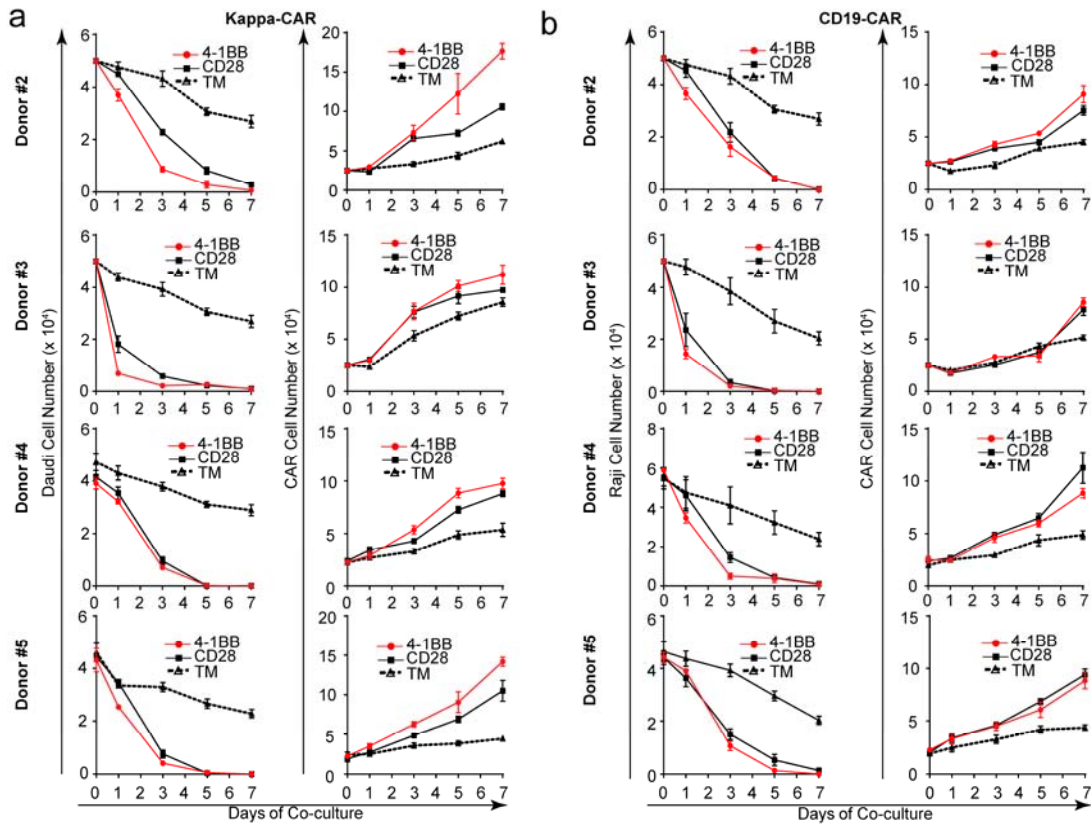


Figure S7: 4-1BB-CAR T cells have enhanced antitumor activity and proliferation measured by long-term killing assays.

(a) Kappa-CAR T cells were isolated from four different individuals and transduced with TM, 4-1BB, and CD28 constructs. The target Daudi cells expressing fluorescent protein mCherry were mixed with CAR T cells for 7 days. The number of both target cells and CAR T cells were measured by flow cytometry, as described in Figure 4. (b) CD19-CAR T cells were isolated from four different individuals and transduced with TM, 4-1BB, and CD28 constructs. The Raji-GFP target cells were mixed with CAR T cells for 7 days. The number of both target cells and CAR T cells was measured by flow cytometry. This data is pooled from at least three independent experiments.

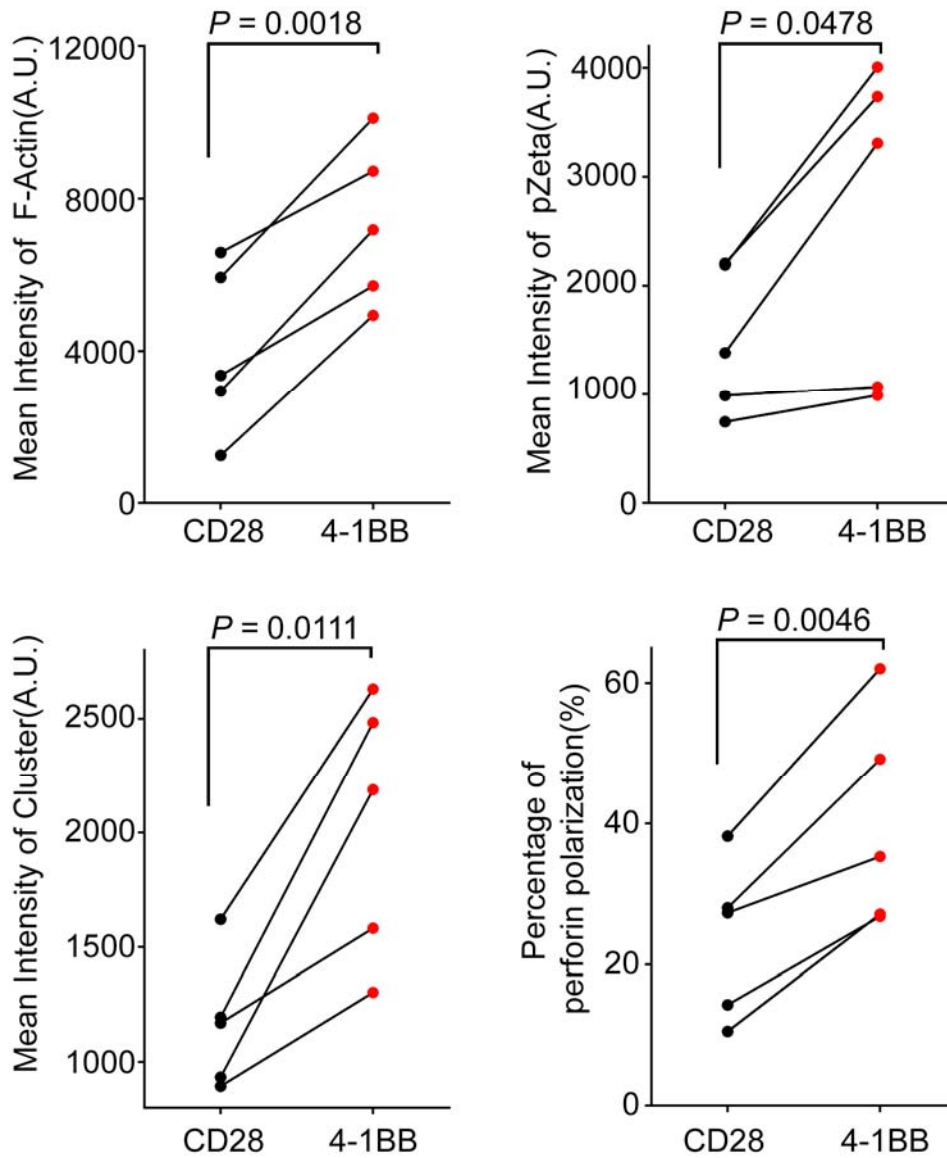


Figure S8: 4-1BB-CAR T cells show higher IS quality from five individuals. PBMCs from five individuals were transduced with Kappa-4-1BB-CAR (red dots) or Kappa-CD28-CAR construct (black dots) retrovirus. The MFIs of F-actin, pZeta, antigen cluster, and percentage of perforin polarization at the IS from Kappa-CAR T cells were calculated. The transduced CAR T cells were activated by lipid bilayers carrying Kappa-Alexa Fluor 647 to quantify the MFI on the plasma membrane to evaluate the IS quality. This data is pooled from at least two independent experiments. *P* value is for paired t-test.

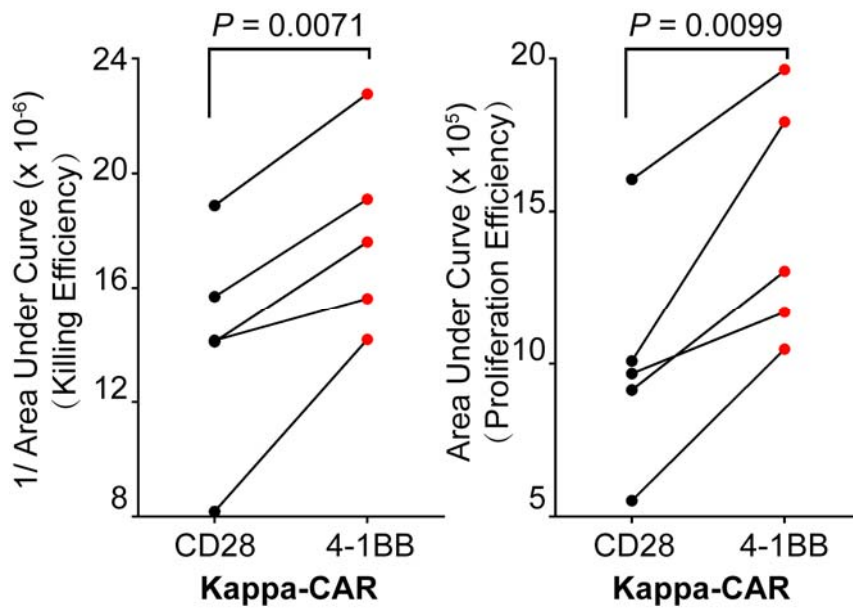


Figure S9: Superior anti-tumor activity from 4-1BB-Kappa-CAR T cells from five individuals. PBMCs from five individuals were transduced with 4-1BB Kappa-CAR (red dots) or CD28 Kappa-CAR (black dots) retrovirus. The reciprocal of the area under the curve of target cell numbers (killing efficiency, left) and area under the curve of effector cell numbers from Kappa-CAR T cells (proliferation efficiency, right) were calculated, respectively. The transduced CAR T cells were activated by co-culturing with a Kappa-positive Daudi cell line to quantify the anti-tumor activity. This data is pooled from at least two independent experiments. *P* value is for paired t-test.

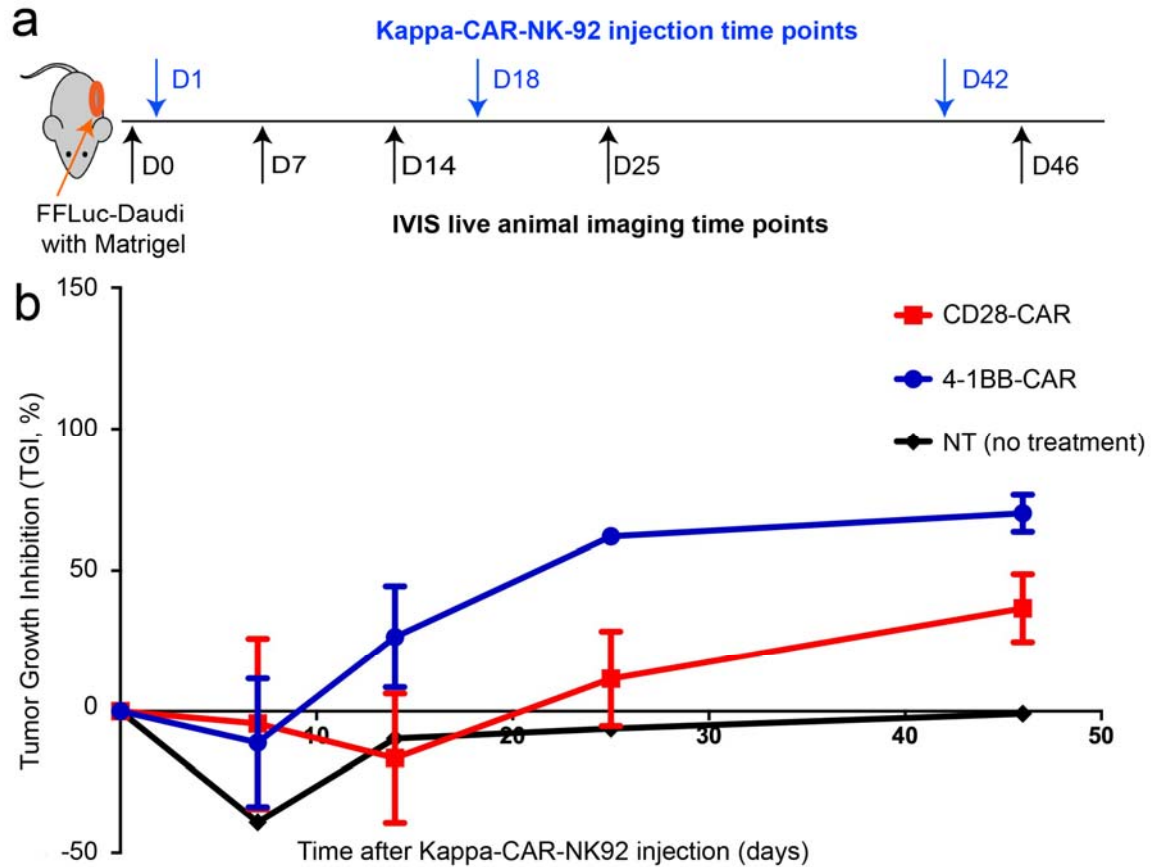


Figure S10: 4-1BB-CAR-Kappa NK-92 cells show superior anti-solid tumor activity *in vivo*. (a) NSG mice ($n=6$) were subcutaneously injected with 2×10^6 luciferase-expressing Daudi (FFLuc-Daudi) cells mixed with Matrigel (Day -7) to mimic solid tumor xenograft animal model. At day 1, mice were injected (i.v.) with one-dose 5×10^6 effector CAR NK-92 cells (CD28 and 4-1BB). As a control, no treatment (NT) group was infused with PBS. On day 18 and 42, all the mice were subjected to intra-tumor injection of the 5×10^6 effector CAR NK92 cells and PBS (as a control). IVIS imaging was recorded using the bioluminescence value (photons/second) at the indicated time points. (b) Tumor growth inhibition (TGI) was calculated, as described previously at indicated time points. Error bars show \pm s.d.